LA-4112

Q.2

LOS ALAMOS SCIENTIFIC LABORATORY
of the
University of California

LOS ALAMOS • NEW MEXICO

Operation of a Radio-Frequency Nuclear Spin Filter

UNITED STATES
ATOMIC ENERGY COMMISSION
CONTRACT W-7405-ENG. 36

This report expresses the opinions of the author or authors and does not necessarily reflect the opinions or views of the Los Alamos Scientific Laboratory.

Printed in the United States of America. Available from
Clearinghouse for Federal Scientific and Technical Information
National Bureau of Standards, U. S. Department of Commerce
Springfield, Virginia 22151
Price: Printed Copy $3.00; Microfiche $0.65

Written: February 1969
Distributed: May 16, 1969

LA-4112
UC-37, INSTRUMENTS
TID-4500

LOS ALAMOS SCIENTIFIC LABORATORY
of the
University of California
LOS ALAMOS • NEW MEXICO

Operation of a Radio-Frequency Nuclear Spin Filter

by

Gerald G. Ohlsen

Joseph L. McKibben

Ralph R. Stevens, Jr.

George P. Lawrence

Ned A. Lindsay

TABLE OF CONTENTS

OPERATION OF A RADIO-FREQUENCY NUCLEAR SPIN FILTER

by

Gerald G. Ohlsen, Joseph L. McKibben, Ralph R. Stevens, Jr.

George P. Lawrence, and Ned A. Lindsay

ABSTRACT

Details of the construction and operation of the nuclear spin filter in conjunction with the Los Alamos Scientific Laboratory Lamb-shift polarized-ion source are presented.

I. GENERAL

This report is one of a series which describes the design, construction, and operation of the Los Alamos Scientific Laboratory (LASL) Lamb-shift polarized negative-ion source. We report the details of the radio-frequency selective quenching device that we call a nuclear spin filter. This device transmits metastable hydrogen, deuterium, or tritium atoms only if the nuclear-spin quantum magnetic number (m_I) corresponds to the one for which it is tuned. Atoms with other spin orientations are quenched to the ground state. The device provides (1) a uniform magnetic field parallel to the beam, (2) a ~1600-MHz radio-frequency electric field parallel to the beam, and (3) a static electric field perpendicular to the beam. It depends on the "three-level interaction" phenomenon discovered by Lamb and Retherford[1] and Lamb.[2] A brief sketch of the theory has been given in Ref. 3, and a detailed account has been published in a report.[4] A paper which describes the application of the theory to the selection of the optimal cavity geometry has been prepared.[5] Only those aspects of the device that are of significance to the practical implementation of the method are presented in this report.

The spin filter is indicated schematically in Fig. 1. A uniform magnetic field is provided by solenoidal windings. The details of the magnetic field design have been described[6] and will not be discussed here. (A homogeneity of about ±0.2 G at 600 G in the spin-filter region, i.e., over a length of 10 in., is achieved by our design.) The overall performance of the spin filter can be described in terms of the efficiency, ϵ, which is defined as follows. In an ideal device, according to the three-level interaction theory, 100% of a beam of α-state metastable atoms (i.e., $2S_{1/2}$, $m_J = +1/2$ atoms) with the selected m_I can be transmitted. Several factors, however, prevent ideal performance; ϵ represents the fraction of α metastable atoms, with the desired m_I, that are actually transmitted.

The presence of the f level (i.e., the $2P_{1/2}$, $m_J = -1/2$ level), with the attendent α-f transitions induced by the transverse dc field, is the major reason for ϵ being less than unity. Some secondary factors that can reduce ϵ are (1) the presence of the e level (i.e., the $2P_{1/2}$, $m_J = 1/2$ level) with the attendent α-e transitions induced by longitudinal dc field components, (2) unwanted α-f transitions induced by transverse rf components, and (3) a variation of the rf or the dc field strength which is too rapid for the atoms to adiabatically follow.[3-5] These effects can be minimized by the

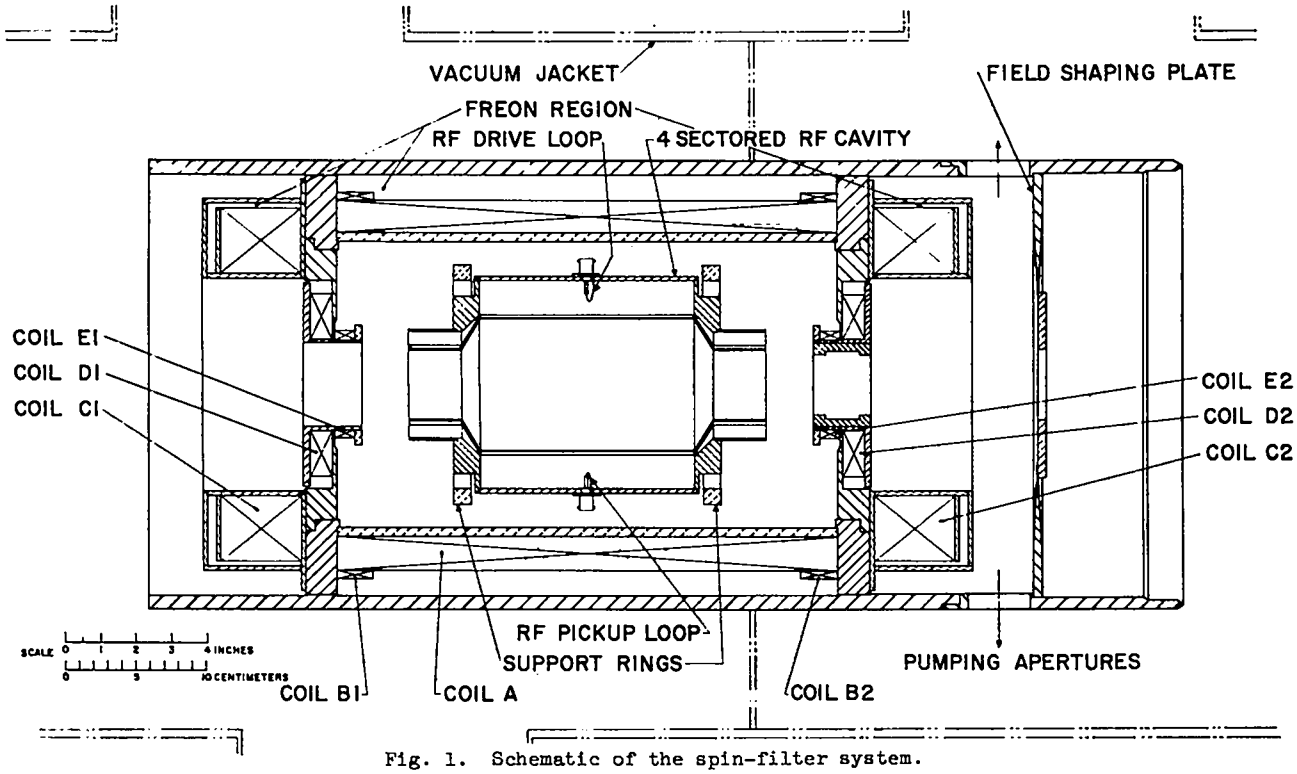

Fig. 1. Schematic of the spin-filter system.

selection of a suitable cavity geometry, as discussed below.

Inadequate magnetic-field homogeneity can also reduce ϵ; therefore, a number of solenoidal coils are provided. The main magnetic field is provided by coil A (Fig. 1). The rising and falling fields, which should have reached low values at a distance of ~12 in. from either end of the cavity, are provided by coils C1 and C2, respectively.[6] Coil pairs B1-B2 and E1-E2 provide trim fields which bring the homogeneity to the required level in the rf cavity region. The coil pair D1-D2 compensates for the perturbations (dips) caused by the 7/8-in.-thick iron annuli which separate coil A from coils C1 and C2.

The features which characterize a good design for the rf cavity are:

1. The maximum possible transmission, ϵ, for α-state atoms with the desired m_I.
2. Zero transmission for all other metastable atoms.
3. A single design for H, D, or T, atoms.
4. Minimum length.
5. Low sensitivity to magnetic field in homogeneity.
6. Simplicity of construction.

The general design that appears to best meet the above requirements consists of a cylindrical cavity with end pipes, as shown in Fig. 1, operated in the TM_{010} mode. The cavity is cut into four sectors and a dc voltage is applied across one pair. For good performance, the rf field is required to rise gradually at each end of the cavity.[5] However, the rate of rise of the rf field strength decreases with increasing end-pipe diameter; this suggests the use of a fairly large diameter. Also, the rate of quenching loss in the end region varies approximately as the inverse square of the diameter, so that a large diameter is again suggested. However, to adequately contain the rf field, the length of the end pipe must be at least 2/3 of its diameter, so the whole device must be made longer if larger diameter end pipes are used. (If the end-pipe length is made shorter than 2/3 of its diameter, the

cavity Q will be sensitive to the placement of external objects. If the end-pipe length is made shorter than about 1 in., a significant decrease occurs in the cavity Q.)

The length of the cavity should be kept as short as possible because the required magnetic-field homogeneity decreases rapidly with the overall length. This decrease arises from two factors. First, the length of time, t, that the metastable atoms are in the cavity is shorter for a shorter cavity, and second, the rf and dc field strengths required for a shorter cavity are both greater. The increased dc field increases the three-level resonance line width and, thus, there is less intrinsic sensitivity to magnetic-field inhomogeneity. For a given inhomogeneity, the transmission loss from this cause varies somewhat faster than linearly with cavity length. If the cavity gets too short, however, adiabatic losses will become serious.

II. CAVITY DESIGN

Extensive numerical studies of the system of differential equations that describe the four-level system[4,5] resulted in a cavity configuration which has a 6-in.-long central section, a 10-in. overall length, and a 3-in.-diam. end pipe. A section beveled at 45° connects the large and the small diameter sections. The cavity is cut into four quadrants; the (adjustable) width of the slot between quadrants is approximately 1/4 in. when the cavity is tuned to 1609 MHz (corresponding to a central region diameter of 5.77 in.). The four quadrants are insulated from the support ring; the dc voltage is applied symmetrically to an opposing pair. The rf cavity is shown in Fig. 2.

The resonant frequency, f, for a TM_{010} mode is controlled solely by the radius, a, of the cylinder and is given by $f = c/(2.61a)$, where c is the velocity of light. For the present cavity, which does not operate in a TM_{010} mode, but rather in a TM_{010}-like mode, we find that $f = c/(2.54a)$, or about 2.6% higher than the TM_{010} frequency for a particular radius. This relation was observed to hold over a range of about 150 MHz. The end openings, not the longitudinal slots, are primarily responsible for this frequency shift.

The end sections are 2 in. long and 3 in. in diameter. These sections operate as wave guides

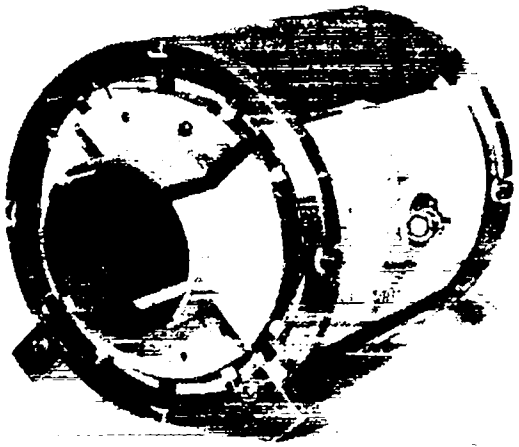

Fig. 2. Photograph of the rf cavity.

below cutoff[7] and, therefore, the rf field drops rapidly to zero in the end-pipe region. However, it was found that a 2-in. or greater length was required to adequately contain the rf power. As mentioned above, a shorter length leads to some power loss, lowered Q, and a sensitivity to the placement of surrounding metal objects. Even with 2-in. end pipes, no metal should be allowed closer than ∿1/2 in. to the cavity end. In the present design, the closest metal parts are the coils E1 and E2, where the spacing is about 1-1/4 in. Plastic and other nonmetal parts are not as undesirable as metal, but still contribute an unacceptable loading effect and should be eliminated.

Three rf properties of the cavity are of interest. First, the shape of the rf field strength vs the position on the axis should be known. Second, the Q of the cavity determines the required frequency stability and power level of the oscillator. Third, the absolute value of the rf fields in terms of a measurable power level should be known.

The rf field profile can be measured by using the Slater perturbation theorem,[8] which states that the frequency of a cavity will be shifted when an object is placed within it, according to the formula

$$\delta = \frac{k \int (\mu_o H^2 - \epsilon_o E^2)\, d\tau}{4U} ,$$

where δ is the fractional frequency change; k is a constant that depends on the geometry of the

perturbing object (= 3 for a sphere); μ_o, H, ε_o, and E have their usual electrodynamic meanings; and U is the total electromagnetic energy in the cavity. The integral is carried out over the volume of the perturbing object. The fields in a pure TM_{010} mode are given by $E_z = E_o J_o(kr)$ and $H_\phi = \frac{E_o}{\eta} J_1(kr)$, where $\eta = \sqrt{\frac{\mu_o}{\varepsilon_o}} = 377\ \Omega$, and $k = 2.405/a$, where a is the cavity radius. All other field components are zero. Thus, along the axis, H_ϕ is zero and E_z has the constant value E_o. If the perturbing object is small enough to allow E(r,z) to be regarded as constant over its volume, $\Delta\tau$, we obtain

$$\delta = \frac{-3\,\varepsilon_o\,E^2\,\Delta\tau}{4U} \quad .$$

Thus, the relative electric field strength is proportional to the square root of the frequency shift. The measured axial rf field distribution, normalized to unity at the cavity center, is shown in Fig. 3. A 3/8-in.-diam. brass ball suspended on a taut nylon line was used to make the measurements.

The absolute power level may also be obtained by using the above formula. The unloaded Q of the cavity, denoted by Q_o, is defined by

$$Q_o = \frac{\omega\,U}{W} \ ,$$

where W is the power loss in the cavity, ω is the angular frequency, and U is again the electromagnetic energy content of the cavity. Using this, we obtain from the perturbation formula

$$\delta = \frac{-3\,\omega\,\varepsilon_o\,E^2\,\Delta\tau}{4\,W\,Q_o} \ ,$$

which can be written as

$$E^2 = \frac{-4\,W\,Q_o}{3\,\omega\,\varepsilon_o\,\Delta\tau} \quad .$$

Using the relation $\delta = \frac{\Delta f}{f} = -\frac{\Delta\lambda}{\lambda}$ and $1/\omega\varepsilon_o\lambda = 60\ \Omega$ (mks units), this becomes

$$E^2 = 80\,W\,Q_o\,\frac{\Delta\lambda}{\Delta\tau} \ .$$

At the center of the cavity, we observed a frequency decrease of 1.617 MHz at an operating frequency of 1608.8 MHz. Thus, $\Delta\lambda = \lambda(\Delta f/f) = 1.875\times10^{-4}$ m. The volume of the probe, $\Delta\tau$, was $4.524\times10^{-7}\ m^3$, so $\Delta\lambda/\Delta\tau = 414.4\ m^{-2}$. Finally, then, we obtain

$$E(V/cm) = 1.820\,\sqrt{Q_o W\ (watts)} \ .$$

The cavity Q_o can be obtained from the loaded Q by the relation

$$Q_o = Q(1 + \beta_1 + \beta_2) \ ,$$

where β_1 is the coupling parameter between the cavity and the equivalent generator that drives it, and where β_2 is the coupling parameter between the cavity and an external load. In this case, the external load consists of a pickup loop connected to a thermistor-type power meter and also to a crystal detector. The area of the drive loop was adjusted until $\beta_1 \approx 1$. This was accomplished by measuring the forward going and returning power in the drive line by means of a dual directional coupler and a thermistor-type power meter; the area of the drive loop was adjusted until the returning power was minimum. Power reflection less than 0.1% was easily attainable; this corresponds to a voltage-standing-wave ratio of ∿1.06. The area of the pickup drive loop was adjusted until a convenient power level for measurement was obtained. The loop size has been adjusted several times, but an adjustment such that the power meter reads 12% of the total power being fed into the cavity is convenient. The pickup loop calibration factor is

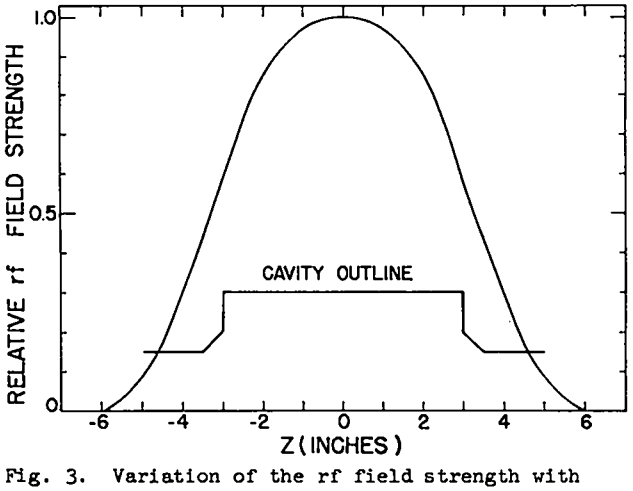

Fig. 3. Variation of the rf field strength with axial position. Note the cavity outline.

determined by first feeding power directly into the (properly terminated) thermistor power-meter head, and then through the cavity and pickup loop into the power-meter head, taking care that the drive loop transmits all of the applied power (i.e., $\beta_1 = 1$). The power ratio, measured as just described, is related to the coupling coefficients β_1 and β_2 by the transmission formula[8]

$$T = \frac{P_L}{P_o} = \frac{4\beta_1\beta_2}{(1+\beta_1+\beta_2)^2} ,$$

where P_L is the power delivered through the cavity to a load and P_o is the power available, at the cavity input, to a matched load. If $\beta_1 = 1$, we can solve this equation for β_2. We find

$$\beta_2 = 2\left[\left(\frac{1-T}{T}\right) \pm \sqrt{\left(\frac{1-T}{T}\right)^2 - 1}\right] .$$

which, for the solution that corresponds to $\beta_2 < 1$, gives $\beta_2 \approx \frac{T}{1-T}$ for small T. Thus, since $T \approx 0.88$, $\beta_2 \approx 0.14$. We now have all the information required to relate the loaded-cavity Q to Q_o: namely, $Q_o = 2.14\ Q$. The half-power points of the system are found to be 175 kHz apart, so that $Q = 1608/0.175 \approx 9{,}200$ and, therefore, $Q_o = 19{,}700$. We finally obtain

$$E(V/cm) = 255\sqrt{W\ (watts)} ,$$

where W is the actual rf power in the cavity; that is, W = (1.0-0.12)/0.12 times the power indicated by the power meter connected to the pickup loop.

The drive and pickup loops are shown in Fig. 4. They consist of ordinary BNC panel-mount female connectors with copper-wire loops soldered to the center pin and to the body of the connector. The loop assemblies can be easily removed; in fact, pickup loops which remove various fractions of the power can be precalibrated and interchanged as desired.

In adjusting the drive-loop area, it is possible to determine whether the loop is too large (overcoupled) or too small (undercoupled) from the nature of the standing-wave pattern. However, it is probably simpler to start with a large loop and reduce the effective area, while observing the reflected power, by turning the connector to couple to fewer and fewer H lines in the cavity. After a few iterations, the correct loop size can be found.

The cavity is cut into four sectors and a voltage is applied across an opposing pair (which do not contain either the drive loop or the pickup loop) to provide the required transverse dc field. The calculated[9] shape of the dc field along the cavity axis is shown in Fig. 5. Two-dimensional geometry was used for the calculation. The approximate variation of the electric field over the cross section of the beam is shown in Fig. 6. This figure is based on calculations[9] of the fields produced by a symmetrically biased, infinitely long, four-sector geometry. The maximum diameter of the metastable beam in our apparatus is about 1-1/2 in.; the dc electric field has good uniformity over this region. The rf electric field varies, for a TM_{010} mode, as $J_o(2.405r/a)$; for r = 0.75 in. and a = 2.88 in., the rf field strength has 91% of its axial value. The rf electric and magnetic field amplitudes vs radius, r, for a TM_{010} mode are shown in Fig. 7.

It is interesting to compare the observed

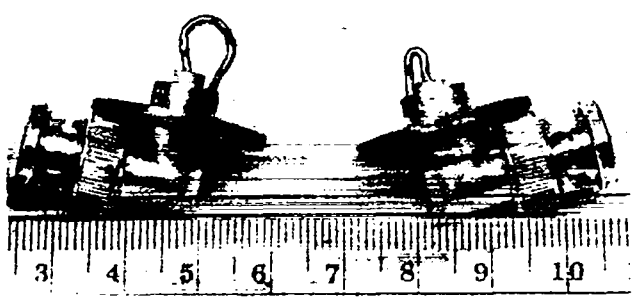

Fig. 4. Photograph of the drive and pickup loops. The scale is in cm.

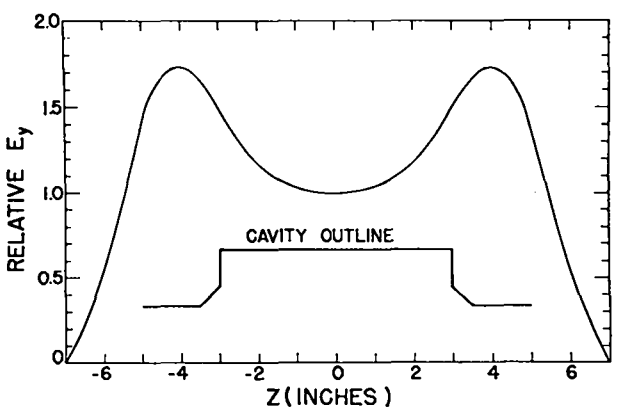

Fig. 5. Variation of the dc field strength with axial position. Note the cavity outline.

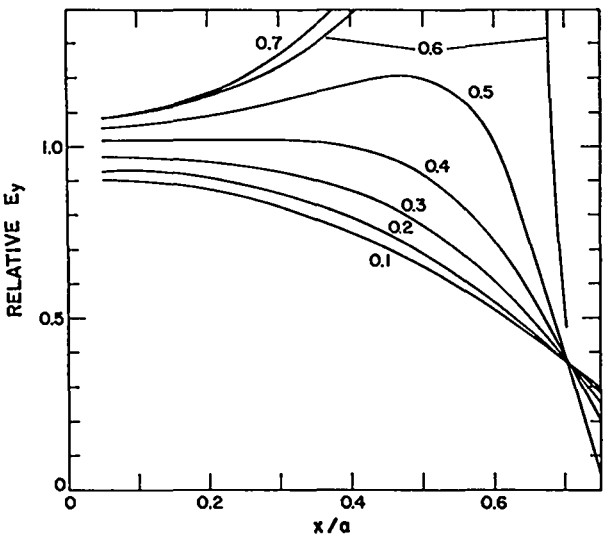

Fig. 6. Graph of relative E_y vs x/a for the values of y/a indicated, where a is the cavity radius.

value of Q_o with the expected value for a TM_{010} mode. The theoretical Q_o of such a cavity may be written[10]

$$Q_o = \frac{\eta}{R_s} \frac{2.405}{2[a/h+1]} \quad (TM_{010} \text{ mode}) ,$$

where $\eta = \sqrt{\frac{\mu_o}{\varepsilon_o}} = 377\ \Omega$, a is the cavity radius, h is the cavity length, and R_s is the surface resistivity of the cavity material. For silver, as used here, $R_s = 2.52\times10^{-7}\sqrt{f}\ \Omega$, where f is the operating frequency. For a = 2.88 in., h = 6 in., and f = 1.6×10^9/sec, we obtain Q_o = 30,400. Thus, our actual Q_o is about 65% of the ideal TM_{010} value. Some of this difference is undoubtedly because our cavity does not resonate with a mode precisely like a TM_{010} mode. We followed the standard practice of plating the copper cavity surface with silver, with a thin layer of rhodium applied over the silver for corrosion protection. Our experience indicates that bare copper is about as good as plated copper.

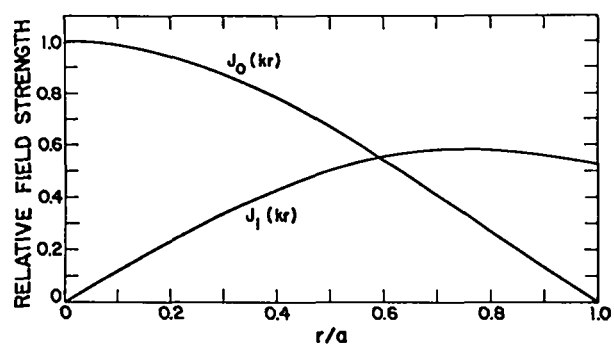

Fig. 7. Graph of $J_0(kr)$ and $J_1(kr)$ vs r/a, where a is the cavity radius, and k = 2.405/a. The rf electric field z component varies as $J_0(kr)$, while the rf magnetic field ϕ component varies as $J_1(kr)$.

III. SYSTEM DESIGN

The cavity was installed in accordance with the block diagram presented in Fig. 8. A 10-W, 1609-MHz oscillator (Trak Microwave Corp., Tampa, Fla., Model 2975-1033) furnishes the rf power. A schematic of the oscillator dc supply is given in Fig. 9. A ferrite isolater (Microlab/FXR, Livingston, N. J., Model N1578) prevents reflected power, which can be appreciable when the cavity is off resonance, from interacting with the source. Power is removed for frequency counting by means of a directional coupler (Hewlett-Packard Model 796D) and counted with a frequency converter (Hewlett-Packard Model 5254B) feeding a 50-MHz frequency counter (Hewlett-Packard Model 5245L). In our initial setup, this was followed by a variable attenuator (Hewlett-Packard Model 394A); the power was then sent to the cavity by means of ~35 ft of RG-8 cable (total attenuation about 6 dB). Power from the pickup loop was sent through 35 ft of RG-8 cable to the thermistor-type power meter (Hewlett-Packard Model 478A thermistor mount and Model 431C power meter) for monitoring. The power-level reading gives all the information required to obtain correct tuning of the oscillator and also to monitor the absolute cavity power level, as discussed above.

Several difficulties with this simple initial system became quickly apparent. First, thermal effects were sufficiently large that the oscillator had to be retuned every few minutes. For a TM_{010} mode, $\delta f/f \approx \delta a/a$; that is, the fractional frequency change varies as the linear expansion coefficient. For brass, this coefficient is about 20 ppm/°C; thus, about 30 kHz/°C is expected. Thermal drifts of at least 10°C occur in the cavity region, but with much longer time constants than a few minutes. Investigation showed that the oscillator itself was the most unstable element. The instability was reduced by mounting the oscillator in a heavy aluminum enclosure which acted as a thermal buffer.

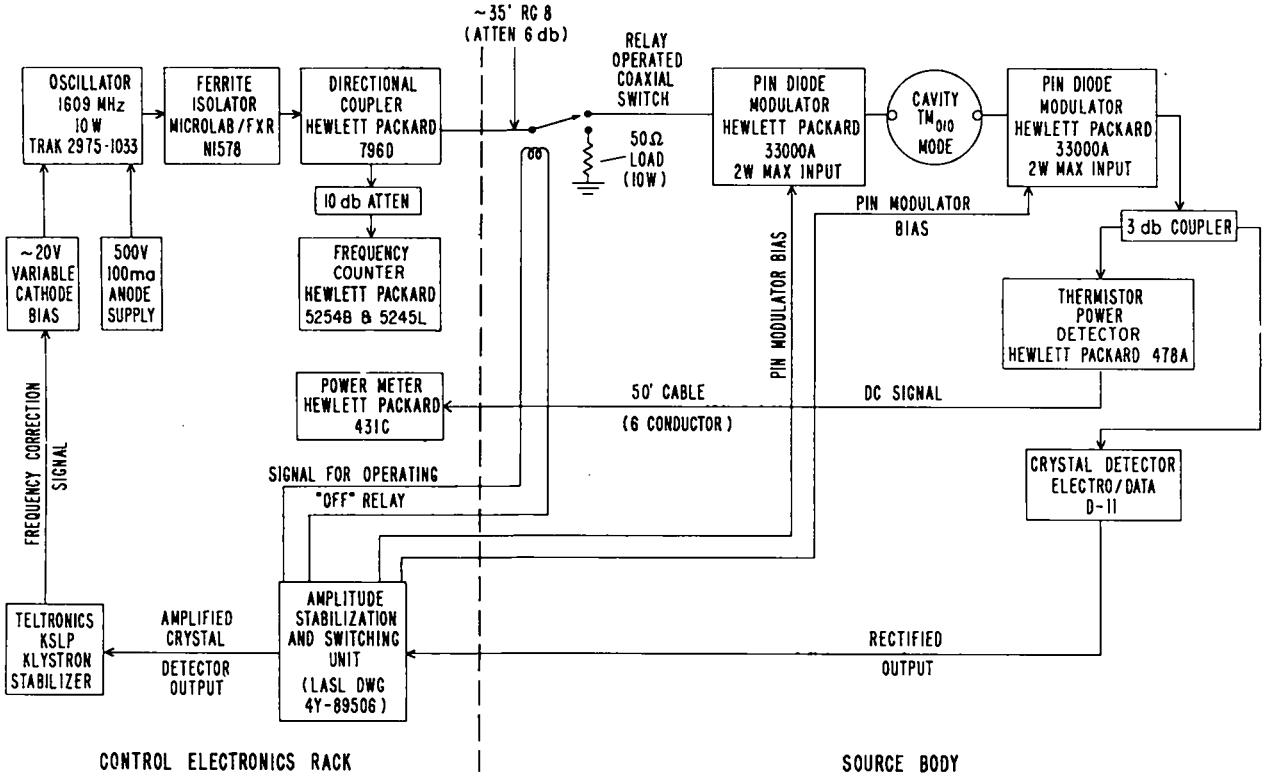

Fig. 8. Block diagram of the rf system.

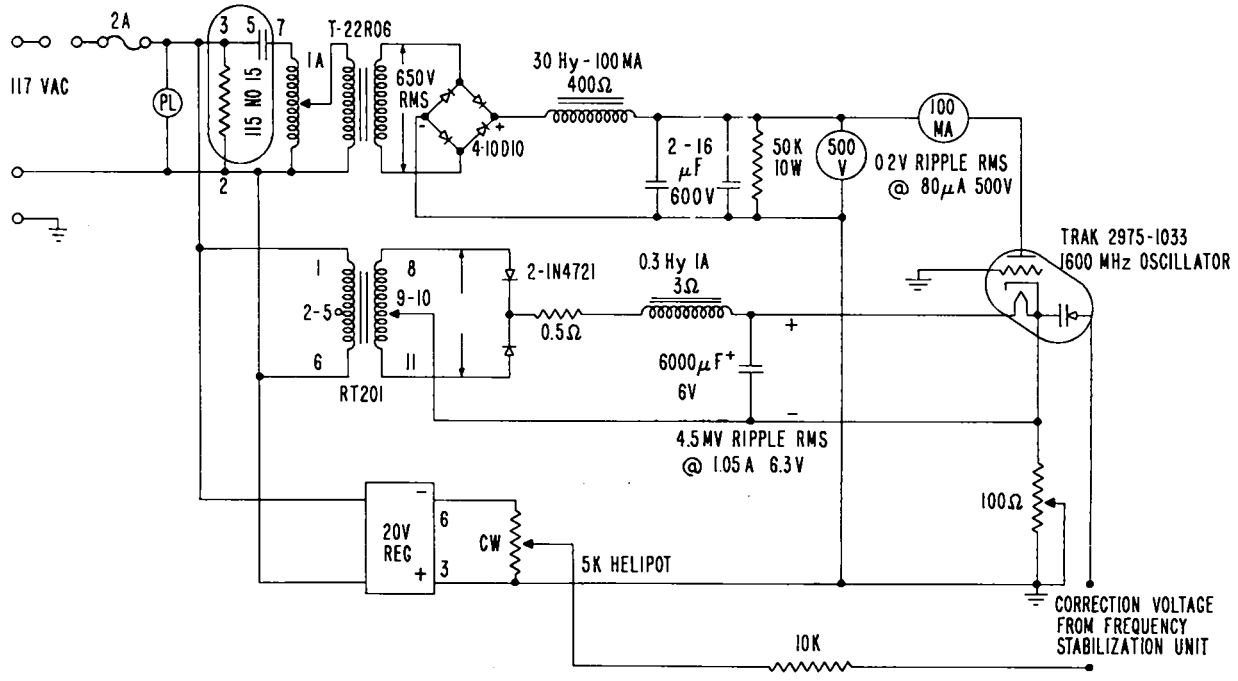

Fig. 9. Schematic of the oscillator dc supply.

Although this improved the situation greatly, and the system was used this way for some time, we felt that frequency stabilization by electronic means was desirable. Fortunately, a commercial unit (Teltronics Inc., Nashua, N. H., Model KSLP) was available which could handle the job. This unit modulates the drive frequency by application of a 70-kHz signal to the grid of the Trak oscillator. The signal transmitted through the cavity is detected by means of a crystal detector and the unit derives a correction signal by comparing the 70-kHz modulation wave to the detected 70-kHz wave. No modification of the commercial unit was required. When this device is used, the power transmitted by the cavity must be divided between a crystal detector and the thermistor detector. A 3-dB splitter is used for this purpose (Microlab/FXR Model 02-2TN). We are using a very sensitive tunnel diode-type crystal (Electro/Data, Inc., Garland, Tex., Model D-11). This detector has a sensitivity such that about 75 mV is delivered into a 1000-Ω load with an input power of 0.15 mW. (The signal level required to operate the frequency stabilizer is approximately 75 mV.)

The power coming from the cavity pickup loop is about 1/7 of the power in the cavity and, thus, the minimum cavity power at which the frequency stabilizer is usable is $\sim 7 \times 2 \times 0.15$ mW, or 2.1 mW. The factor 2 arises from the 3-dB splitter that divides the power between the crystal and the thermistor. This corresponds to an rf field strength of ∿11 V/cm, which is approximately the correct operating level. We consider it desirable, however, that fields as low as 5 V/cm be attainable, even though theory indicates that field strengths between 10 and 20 V/cm are required.

Larger signals for regulation can be obtained by increasing the size of the pickup loop. However, this will decrease the maximum power available in the cavity. Fields as high as several hundred V/cm are needed to guarantee full quenching of all metastable atoms. With the minimum attenuation in the attenuator (6 dB) and the 6 dB of unavoidable losses in the drive line, together with the fact that the oscillator sometimes puts out less than its rated power, the available power was found to be marginal (∿300 mW), even with only 12% loss to the detector. Since the frequency stabilization unit will operate with ∿1/4 of the design signal level, the above arrangement is operable to about 5 V/cm and, therefore, is usable. However, for increased flexibility, we inserted an amplifier (gain of 10) between the crystal and the frequency stabilizer unit. This amplifier is an integral part of the amplitude stabilization unit discussed in Sec. IV.

IV. AMPLITUDE SWITCHING AND STABILIZATION

When the spin-filter magnetic field is near the value for which the electron cyclotron frequency corresponds to the 1609-MHz cavity frequency (∿575 G), significant power absorption occurs. This is of no consequence for hydrogen atom operation, where the two resonances are at ∿535 G ($m_I = 1/2$) and ∿605 G ($m_I = -1/2$). However, it is a major inconvenience for deuterium atoms, where the resonances occur at ∿565 G ($m_I = 1$), ∿575 G ($m_I = 0$), and ∿585 G ($m_I = -1$). This absorption occurs over at least a 10-G range, so that it has some effect on the operation with $m_I = \pm 1$, and it has a very large effect on $m_I = 0$ operation. The extent of the absorption, which goes as high as 98%, also depends on the intensity and character of the charged beam entering the spin filter; thus, the loading effect is expected to be time-dependent.

For the above reason, and also because of the slow drifts in the power output of the oscillator, we decided that a power-leveling device would be useful, especially when the ion source goes into routine operation. It is also desirable to provide a means for rapidly switching the power level between two selectable levels, the first for ordinary operation (∿1 mW in the cavity), and the second for full quenching of the metastable beam (>300 mW in the cavity). The beam polarization is directly related to the ratio of the output ion currents obtained from the source under these two conditions.[11] Prior to construction of the device about to be described, this power-level switching function was accomplished with a fixed attenuator which was mechanically switched, with coaxial switches, from just before the drive loop to just beyond the pickup loop. If a 20-dB attenuator were used, for example, the cavity power level would change by a factor of 100 while the power-meter reading would remain about constant. Thus, the operator could maintain proper tuning on either setting.

The rf power-leveling system uses PIN diode modulators (Hewlett-Packard Model 33000A) before and after the cavity. It allows switching between high and low settings, and power leveling in either setting. Near 575 G, power leveling in the high setting is generally not possible because sufficient power is not available.

The circuit operates basically as follows (Fig. 10). The output attenuator is operated with a fixed bias current, switchable from high to low setting with SW 1, so that it operates as a fixed attenuator. The power level, as measured by the diode detector, is compared to the desired reference level, and an appropriate correction is generated if these do not agree. A 100-Hz low-pass filter is incorporated into the system to avoid difficulty with control-loop oscillations, and also to avoid interaction with the 70-kHz modulation imposed by the frequency stabilizer. Unfortunately, this causes the system to respond too slowly to adjust to transient phenomena induced by sparks.

The bias amplifier and low-pass filter in the output modulator control circuit do not serve any function at present, but were included for flexibility before the exact requirements were known. It would be possible, for example, to modulate the cavity power by applying a suitable signal to this branch of the system.

The drive circuits must deliver up to 200 mA (i.e., up to the maximum rated bias current for the modulators). A current meter measures each of these currents; these serve mainly as indicators so that one can easily recognize which state the system is in (i.e., "high" or "low" power), and whether or not appreciable loading effects are present.

Figure 11 shows a detailed schematic of the circuit. The dc power supplies used in the device are described in Table I. All differential amplifiers are inexpensive units with an open-loop gain

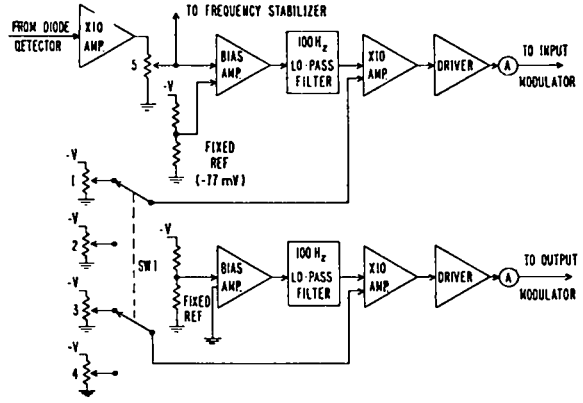

Fig. 10. Block diagram of the switching and leveling circuit.

of 2300 and an open-loop bandwidth of 1.1 MHz (Fairchild Semiconductor, Mountain View, Calif., Model 712C).

The main control switch has four positions. In position 1, a relay, which shunts all of the rf power into a dummy load, is closed. The resulting zero cavity power is useful for studying the spin-filter efficiency, ϵ. Position 2 corresponds to the low rf setting, position 3 corresponds to the high rf setting, and position 4 corresponds to "maximum power," in which the input attenuator is biased for minimum attenuation. Of course, no regulation is possible in position 4 since the modulator is fully biased. After the system is operating, adjustment of the power level over a small range (a factor of 2 or 3) is best accomplished with the potentiometer, the output of which connects to the frequency stabilizer (potentiometer No. 5 in Fig. 10). The role of switch positions 2 and 3 can be reversed by interchanging the adjustments of potentiometers 1 and 3 with those of 2 and 4. Considerable care is required when setting up to avoid exceeding the maximum power ratings of the attenuators and of the power measurement devices.

TABLE I: dc POWER SUPPLIES

Manufacturer	No.	Max Cur (mA)	Voltage	Ripple (%)	Regulation (%)
Electronic Research†	TR5A	200	5-10	0.05	0.5
Electronic Research	TR10A	200	10-20	0.5	0.5
Electronic Research	TR20A	150	20-30	0.05	0.5

†Electronic Research Associates, Inc., Cedar Grove, N. J.

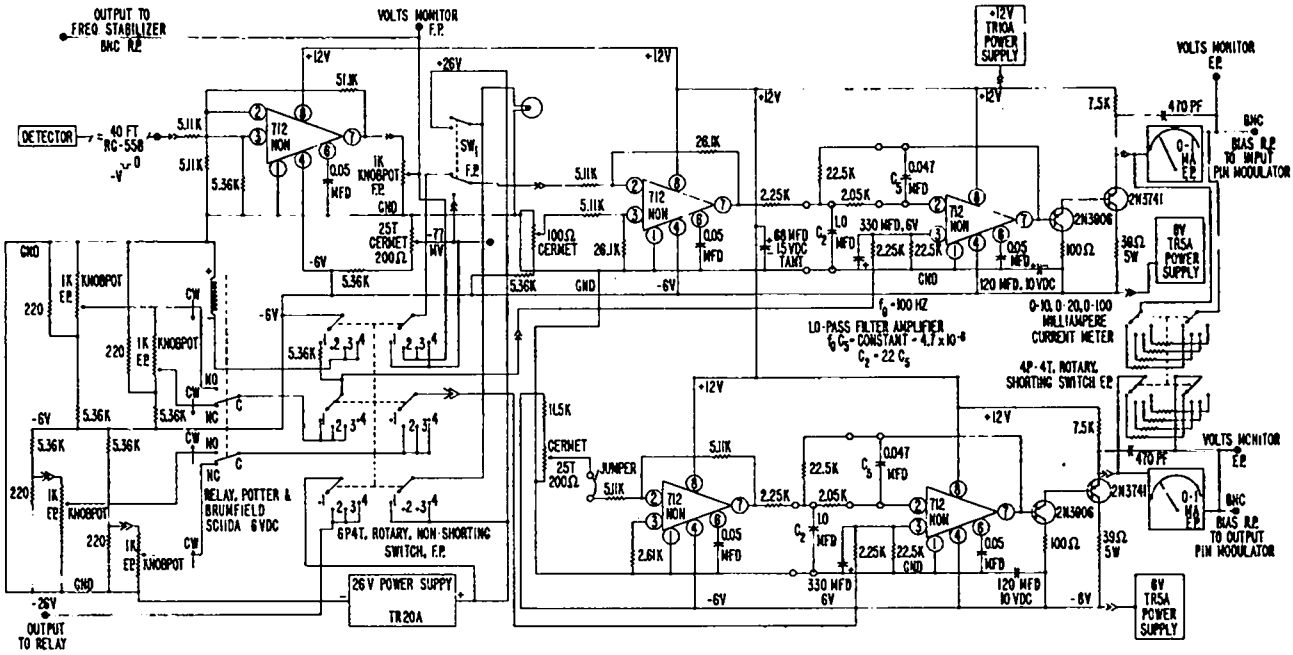

Fig. 11. Schematic of the switching and leveling circuit.

ACKNOWLEDGMENTS

We would like to acknowledge the many discussions with Joseph Parker which have aided materially in our selection of suitable rf components. We also thank Jim Potter for providing test equipment and for advising us regarding the rf cavity measurements. Discussions with Ed Knapp were useful in arriving at our basic cavity concept.

REFERENCES

1. W. E. Lamb, Jr., and R. C. Retherford, Phys. Rev. 81, 222 (1951).
2. W. E. Lamb, Jr., Phys. Rev. 85, 259 (1952).
3. J. L. McKibben, G. P. Lawrence, and G. G. Ohlsen, Phys. Rev. Letters 20, 1180 (1968).
4. G. G. Ohlsen and J. L. McKibben, "Theory of a Radio-Frequency 'Spin Filter' for a Metastable Hydrogen, Deuterium, or Tritium Atomic Beam," LA-3725, Los Alamos Scientific Laboratory (Oct. 24, 1967).
5. G. G. Ohlsen, G. P. Lawrence, and J. L. McKibben (to be published).
6. G. G. Ohlsen, J. A. Jackson, J. L. McKibben, and G. P. Lawrence, "Design of a Solenoid for a Lamb-Shift Polarized-Ion Source," LA-4082, Los Alamos Scientific Laboratory (Mar. 27, 1969).
7. E. G. Linder, I.R.E. Proc. 30, 554 (1942).
8. E. L. Ginzton, Microwave Measurements (McGraw Hill Book Co., Inc. New York, 1957), Chaps. 9 and 10.
9. J. K. Hayes, "The LAPLACE FORTRAN Code," LA-4004, Los Alamos Scientific Laboratory (Sept. 9, 1968).
10. American Institute of Physics Handbook, Second Edition, (McGraw Hill Book Co., Inc., New York, 1963), Section 5, p. 66.
11. G. G. Ohlsen, J. L. McKibben, and G. P. Lawrence, Bull. Am. Phys. Soc., Series II, 13, 1443 (1968).